Raman-scattering study of the electron-phonon interaction in M_3C_{60} (M = K,Rb)

Ping Zhou, Kai-An Wang, and P. C. Eklund
Center for Applied Energy Research and Department of Physics and Astronomy, University of Kentucky, Lexington, Kentucky 40511

G. Dresselhaus
Francis Bitter National Magnet Laboratory, Massachusetts Institute of Technology, Cambridge, Massachusetts 02139

M. S. Dresselhaus
Department of Electrical Engineering and Computer Science and Department of Physics, Massachusetts Institute of Technology, Cambridge, Massachusetts 02139

(Received 2 April 1993)

Temperature (T) -dependent Raman scattering from C_{60}^{3-} intramolecular modes and simultaneous electrical resistivity measurements were made on Rb_3C_{60} films which exhibited a superconducting transition temperature $T_c = 28$ K. K_3C_{60} films were studied for comparison, but at $T = 300$ K only. Weak, or no T dependence in the intramolecular modes is observed through T_c, consistent with the fact that the mode frequencies $\omega > 2\Delta$ (superconducting gap). By comparing the linewidths of the modes in M_3C_{60} to values in pristine C_{60} we have estimated their contributions to the electron-phonon coupling constant λ. Values of λ have been found to be 0.6 and 0.5 for K_3C_{60} and Rb_3C_{60}, respectively, in good agreement with the theoretical value $\lambda = 0.6$ obtained previously by Schlüter and co-workers. The $H_g(2)$-derived mode is found to make the dominant contribution to λ. A line-shape analysis of the $H_g(1)$-derived mode suggests that this mode is a Breit-Wigner-Fano resonance. The radial $A_g(1)$-derived mode linewidth in Rb_3C_{60} is anomalously narrow (~ 0.1 cm^{-1}), and found to be very sensitive to sample quality, i.e., strongly correlated with the width of the superconducting transition.

INTRODUCTION

Since the reports of moderately high-temperature superconductivity in solid $M_{3-x}M'_xC_{60}$ (M, M' = alkali metals),[1-4] there has been substantial theoretical and experimental effort to understand the physical origin of the pairing mechanism in these materials.[5-11] A number of theoretical calculations[5-8] and normal-state Raman-scattering studies of M_3C_{60} (Refs. 9–11) suggest that the interaction between the conduction electrons and the H_g-symmetry intramolecular Raman-active modes may be important to the electron pairing. In this work, we present results of a Raman-scattering study of M_3C_{60} in the superconducting state. Our results confirm the importance of these modes in the pairing mechanism, and furthermore reveal only weak temperature dependence in the H_g mode frequencies and linewidths through the superconducting transition temperature T_c.

Tunneling studies by Zhang and co-workers[12,13] have shown that K_3C_{60} [$T_c = 19$ K (Ref. 1)] and Rb_3C_{60} [$T_c = 29$ K (Ref. 2)] exhibit an energy gap (2Δ) in the superconducting density of states of ~ 68 cm^{-1} or $(2\Delta/kT_c) \sim 5.2$ and ~ 105 cm^{-1} or $(2\Delta/kT_c) \sim 5.3$, respectively, indicating that K_3C_{60} and Rb_3C_{60} may be strongly coupled BCS superconductors. Oshiyama and Saito, also supporting a BCS model,[14] have argued that the difference in T_c between the K- and Rb-doped C_{60} superconductors is primarily due to the differences in $N(\varepsilon_F)$, the electronic density of states at the Fermi level. Because of the weak van der Waals bonding between molecules in pristine C_{60}, four types of vibrational modes might be involved in the pairing mechanism:[15,16] (i) librational modes ($10 < \omega < 30$ cm^{-1}); (ii) low-frequency ($20 < \omega < 70$ cm^{-1}) phonons involving the relative movement of C_{60} molecules against each other; (iii) high-frequency optical phonons ($50 < \omega < 150$ cm^{-1}) corresponding to motion between M^+ ions and C_{60}^{3-} anions; and (iv) intramolecular vibrational modes ($250 < \omega < 1600$ cm^{-1}).

Experiments such as ^{13}C isotope effect studies and inelastic neutron scattering in M_3C_{60} have been carried out to determine which of these groups of vibrational modes [(i)–(iv)] might be important to the pairing mechanism. A wide range of δT_c values for the decrease in T_c due to the ^{13}C isotope effect have been reported ($0.5 < \delta T_c < 1.5$ K).[17-19] Converting these δT_c's into the conventional isotope effect parameter α appropriate for phonon-mediated pairing, values in the range $\alpha \sim 0.3$–0.4 (Refs. 17 and 18) to $\alpha \sim 1.4$ (Ref. 19) are obtained. Although the difference in the experimental α values needs to be reconciled, all ^{13}C isotope effect experiments seem to suggest that carbon modes are involved in the electron pairing. As pointed out by Ebbesen *et al.*,[19] values for $\alpha > 0.5$ are difficult to explain in terms of a conventional electron-phonon coupling mechanism. However, a recently proposed electronic mechanism for the pairing in M_3C_{60} predicts δT_c in the range $0.2 < \delta T_c < 0.6$ K for 100% ^{13}C substitution.[20] Results of an elastic neutron-scattering study of the vibrational modes of M_3C_{60} by Prassides *et al.*[21] have shown that the intramolecular $H_g(2)$ and $H_g(8)$-derived

modes disappear in the spectrum for K_3C_{60}, indicating that these modes are strongly coupled with t_{1u} electrons. The $H_g(1)$, $H_g(3)$, and $H_g(4)$-derived modes in their work only exhibit slightly reduced intensities and increased line broadening, indicating weaker electron-phonon coupling. Nevertheless, their experimental results indicate that the intramolecular vibrational modes of C_{60} might play an important role in the pairing mechanism.

EXPERIMENTAL DETAILS

The carbon soot containing fullerenes was generated using an ac arc method.[22] Details of our adaptation of the process, the subsequent fullerene extraction and purification have been given elsewhere.[23] The M_3C_{60} films were grown in a turbo-pumped vacuum deposition chamber ($p < 1\times10^{-6}$ torr) residing in a He glove box (< 1 ppm of O_2 and H_2O) by sequentially depositing a three-layer sandwich ($C_{60}/M_4/C_{60}$) on quartz substrates. M (C_{60}) was evaporated (sublimed) from separate W boats at ~5 Å/sec (~1 Å/sec). Excess alkali metal in the central layer was found necessary to compensate for apparent loss of the metal to the internal surfaces of the sample cell. For temperature-dependent Raman scattering and electrical resistivity (ρ) studies, an optical cell was constructed which had two parallel quartz windows separated by a stainless-steel ring spacer with In o-rings on its opposite sides to provide a tight seal. One of the cell windows also served as the substrate and had four copper pins silver-epoxied into holes in the substrate, prior to the film deposition. These pins provided electrical contact in a van der Pauw geometry for ρ measurements. The film/substrate was removed from the deposition chamber and the optical cell was assembled in ~1 min inside the He-atmosphere glove box. M_3C_{60} films in this cell can be handled indefinitely in room air without sample degradation, while, for example, the cell is mounted in the cryostat. Whereas the ($C_{60}/K_4/C_{60}$) films had to be annealed at 100 °C for ~10 h to exhibit the characteristic Raman spectrum of a homogeneous M_3C_{60} phase,[11] the ($C_{60}/Rb_4/C_{60}$) films appeared to approach very rapidly (e.g., in minutes) the M_3C_{60} phase without further annealing. The film quality was initially checked by monitoring at $T = 300$ K the downshift of the $A_g(2)$ pentagonal pinch (PP) mode at 1469 cm^{-1} in pristine C_{60} (Ref. 23) to ~1449 cm^{-1}, a characteristic frequency for pure M_3C_{60}.[24]

Superconductivity was observed resistively in the Rb_3C_{60} samples with $T_c = 28$ K. The normal state resistivity near $T = 300$ K was found to be ~12 mΩ cm, consistent with a value of 10 mΩ cm reported previously for Rb_3C_{60} films.[24] The transition width is ~8 K (defined here as the temperature difference between the $0.1\rho^*$ and $0.9\rho^*$, where ρ^* is the resistivity just above the onset of the superconducting transition). This width is broader than that reported for single-crystal studies,[25] but comparable to that reported for film samples.[1] A linear dependence of ρ on T above the transition temperature T_c has been frequently observed in our Rb_3C_{60} films, indicating metallic characteristics of the samples. In the specific sample from which the Raman data presented here were taken, a small effect on ρ, perhaps due to granularity in the films, is identified with the slight upturn of ρ for temperatures T just above T_c.

Raman-scattering experiments were carried out using the 4880- and 5145-Å lines of an argon-ion laser in the Brewster angle backscattering geometry. A cylindrical lens was employed to create an illuminated stripe (0.1×2 mm^2) on the sample surface. A Spex model 1402 double holographic grating monochromator with a dry ice-cooled photomultiplier (ITT FW 130) was used to collect the Raman spectra. Polarization analysis of the scattered light was carried out using a polaroid sheet and subsequent polarization scrambler. The samples were cooled in a closed cycle He refrigerator (CTI-Cryogenics).

RESULTS AND DISCUSSION

In Fig. 1, we plot the room-temperature Raman spectra for C_{60}, K_3C_{60}, Rb_3C_{60}, K_6C_{60}, and Rb_6C_{60} films. In the C_{60} spectrum at the top of the figure, ten strong Raman lines are observed, two polarized A_g and eight unpolarized H_g lines, consistent with group-theoretical predictions for an isolated C_{60} molecule, and thus indicating the weak nature of the intermolecular bonds between nearest-neighbor C_{60} molecules. In the cases of the insulating, M-saturated compounds, e.g., K_6C_{60} and Rb_6C_{60} at the bottom of Fig. 1, there are ~13 strong Raman lines observed, some of which are doublets which can be resolved at higher resolution.[26] Note that the K_6C_{60} and

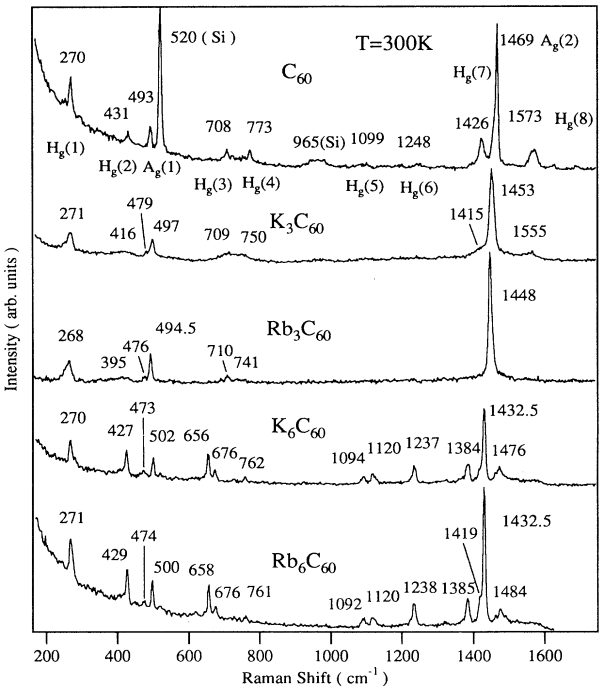

FIG. 1. Raman spectra of C_{60}, K_3C_{60}, Rb_3C_{60}, K_6C_{60}, and Rb_6C_{60} at $T = 300$ K.

Rb_6C_{60} spectra are essentially identical to each other, an experimental fact which has been identified both with a decoupling of the negatively charged C_{60} molecules from the positive M sublattice as well as a total electric charge transfer to form M^+ cations and C_{60}^{6-} anions.[27]

In the center of Fig. 1 the spectra of K_3C_{60} and Rb_3C_{60} are displayed. Similar to the case of the M_6C_{60} compounds, these spectra are also relatively insensitive to the choice of alkali-metal ion species, again indicating both a weak coupling between the C_{60}^{3-} and M^+ sublattices and a complete charge transfer from the alkali-metal atoms to the C_{60} molecules. The most obvious character of these M_3C_{60} spectra in Fig. 1 is the fact that significantly fewer Raman lines are observed than that in other spectra. This could, of course, be attributed to a shorter optical penetration depth. However, the high- and low-frequency A_g-derived modes at ~ 500 and ~ 1450 cm^{-1} are easily detected in the M_3C_{60} spectra, indicating that the incident laser radiation penetrates sufficiently deep into the film to be able to see most, if not all, of the other strong H_g-derived lines. Only three or four of the six strong H_g-derived lines can be observed, and they are significantly broadened. As first proposed by the AT&T group,[5,9] we also associate the missing H_g modes with a line broadening phenomenon which renders these modes difficult to resolve relative to the background. Furthermore, the 268-cm^{-1} H_g mode in both K_3C_{60} and Rb_3C_{60} exhibits an asymmetric line shape characteristic of a Breit-Wigner-Fano (BWF) resonance. This symmetry is shown more clearly in Fig. 2, where the polarized ($\|,\perp$) data[28] are presented with higher resolution and on an expanded frequency scale. Solid lines represent a least-squares fit to a BWF line shape. The

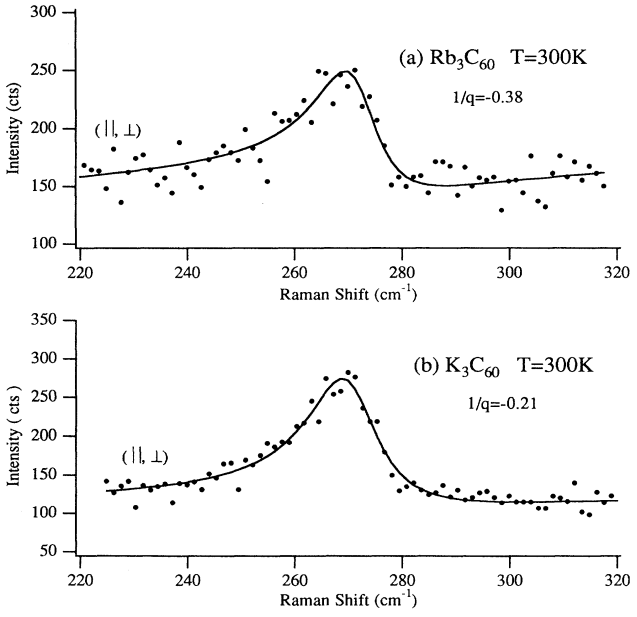

FIG. 2. The $H_g(1)$ model (Ref. 28) for (a) Rb_3C_{60} and (b) K_3C_{60} at $T=300$ K. Solid lines represent the least-squares fit to the Breit-Wigner-Fano line shape.

BWF line shape for the $H_g(1)$ mode was first reported for K_3C_{60},[11] and the present work suggests this may well be a general feature of M_3C_{60} compounds. Briefly, the BWF line shape may be of particular significance because it might also signal, as well as measure quantitatively, the coupling between t_{1u} electrons and the $H_g(1)$ mode. We discuss this point later in more detail. For comparison, the 270-cm^{-1} mode in the Rb_6C_{60} spectrum is actually a doublet with the lines split by ~ 6 cm^{-1}, as seen in higher resolution, and identified with a solid-state interaction.[11,27]

In metals, two scattering channels usually contribute to the Raman linewidth: a two-phonon decay channel and the electron-phonon scattering channel. The former is associated with the anharmonic crystal potential. Recent second-order Raman-scattering studies of solid C_{60} indicate that this anharmonic interaction is fairly small.[29] In the Raman studies on high-T_c cuprates, Cooper and Klein invoked the electron-phonon channel to explain their observations of significant temperature-dependent changes through T_c in the linewidths of several modes.[30] Early experimental Raman-scattering investigations of M_3C_{60} (Refs. 9–11) have attributed the large line broadening of the H_g-derived modes observed in the room-temperature M_3C_{60} Raman spectra to a t_{1u}-derived electron-H_g mode coupling, i.e., an "on-ball interaction." In fact, the broadening of the Raman modes can be used as a measure of the electron-phonon coupling strength.[5,15]

The phonon linewidth broadening ($\Delta\Gamma$) due to the electron-phonon interaction in a metal can be related to a dimensionless electron-phonon coupling constant λ given by[5,15,31]

$$\lambda=\sum_i \lambda_i=\sum_i C\frac{\Delta\Gamma_i}{\omega_i^2}\left[\frac{1}{N(\varepsilon_f)}\right], \tag{1}$$

where ω_i is the unrenormalized discrete phonon frequency for the ith mode, $C=d_i/\pi$, and d_i is the degeneracy of the ith mode. We next apply Eq. (1) to determine experimentally a measure of $\lambda \propto \sum_i \Delta\Gamma_i/\omega_i^2$. This will require a line-shape analysis of the Raman spectra to determine the linewidth broadening $\Delta\Gamma_i$, taken here to be the difference in the full widths at half maximum (FWHM) intensity for the respective A_g or H_g modes in pristine C_{60} and M_3C_{60}.

In Figs. 3(a) and 3(b) we show the results of a line-shape analysis of the Raman spectra for Rb_3C_{60} and K_3C_{60} films at room temperature. The data for the Rb_3C_{60} film are perhaps more meaningful, since this particular film was shown to superconduct for $T<T_c\sim 28$ K. The $H_g(1)$ line was fit to a BWF line shape, and all other modes to a Lorentzian line shape. The results of the Raman line-shape analysis are gathered in Table I. We find that the overall broadening ($\Delta\Gamma$) in K_3C_{60} is somewhat larger than in Rb_3C_{60}. This may well be due to inhomogeneous M doping rather than to an intrinsic linewidth difference. Note also that the strongest line [$A_g(2)$] has a mode frequency 5 cm^{-1} lower in the Rb_3C_{60} spectrum than in the K_3C_{60} spectrum. Since the Rb_3C_{60} film exhibit a $T_c\sim 28$ K, the $A_g(2)$ mode frequency for this sample should be considered a more reliable

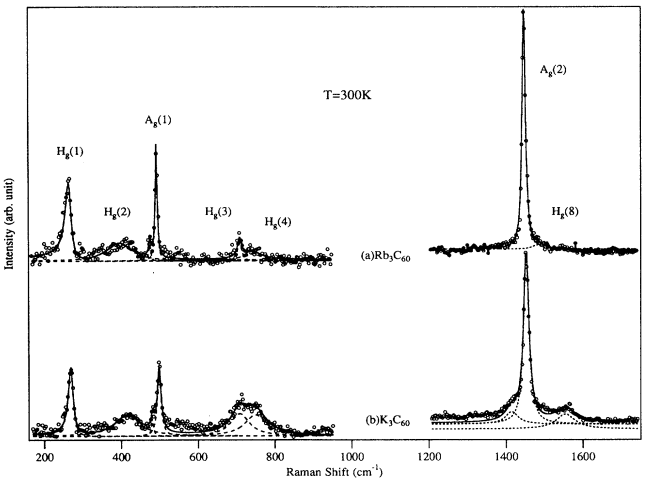

FIG. 3. Line-shape analysis for the Raman spectra ($T=300$ K) of (a) Rb_3C_{60} and (b) K_3C_{60}. Dashed lines represent composite functions used to fit the discrete Raman lines and solid lines represent the summation of all the functions.

value for the M_3C_{60} compounds. In fact this value is consistent with the downshift ~ -6.1 cm^{-1}/M atom for M_3C_{60} and M_6C_{60} compounds.[32] Furthermore, it should be mentioned that our Raman/resistivity studies of several Rb_3C_{60} samples indicate that a linewidth at $T=300$ K of the radial $A_g(1)$ mode (~ 500 cm^{-1}) in excess of ~ 0.5 cm^{-1} was always found to be associated with noticeable broadening of the resistive transition to the superconducting state. The radial $A_g(1)$ mode for the Rb_3C_{60} sample in Fig. 3(a) exhibited a FWHM of only ~ 0.1 cm^{-1} at $T\sim 300$ K, after correcting the data for the instrument resolution. It is also interesting that this linewidth for Rb_3C_{60} is significantly less than the typical linewidth (~ 2–3 cm^{-1}) observed for pristine C_{60} at $T=300$ K.[26,27]

The individual contributions to λ from each Raman-active mode are listed in Table I in the column $\Delta\Gamma_i/\omega_i^2$. It can be seen from Eq. (1) that the low-frequency modes, given equal line broadening, will contribute most to the electron-phonon coupling constant λ. In agreement with the results of Mitch, Chase, and Lannin[10] on ultrathin Rb_xC_{60} films, the $H_g(2)$ mode dominates the contribution to λ, yielding over 60% of the total value for both K_3C_{60} and Rb_3C_{60}. From our results, the $A_g(1)$ mode is apparently not coupled significantly to the t_{1u} electrons, whereas the $A_g(2)$ mode exhibits a measurable broadening (Table I), as predicted recently by Schlüter *et al.*[7] The very narrow linewidth of the $A_g(1)$ mode in Rb_3C_{60} relative to that observed in C_{60} indicates that a substantial reduction in the anharmonic contribution to the mode linewidth has occurred upon doping to $x=3$. We feel this observation deserves further study.

Within the BCS framework, which is not yet definitely established for M_3C_{60} superconductors, we can convert the experimental values for λ into a value for T_c, as done previously.[7,10] This conversion proceeds according to the well-known BCS results given by the McMillan equation

$$T_c=\frac{\hbar\omega_{\ln}}{1.2k_B}\exp\left[\frac{-1.04(1+\lambda)}{\lambda-\mu^*-0.62\lambda\mu^*}\right], \tag{2}$$

where $\omega_{\ln}$ is the logarithmic average over all phonon frequencies weighted according to the coupling to the conduction electrons, k_B is the Boltzmann constant, λ is the electron-phonon coupling constant [Eq. (1)], and μ^* is the Coulomb repulsion between conduction electrons. To evaluate T_c, we have used values for μ^*, $\omega_{\ln}$, and $N(\varepsilon_f)$ from Schlüter's work,[15] i.e., $\mu^*\approx 0.1$, $\omega_{\ln}\approx 1300$ cm^{-1}, and $N(\varepsilon_f)=15$ states/eV spin C_{60}, where $N(\varepsilon_f)$ represents a rough average over several experimental values and theoretical calculations: 1–2 states/eV spin C_{60} from photoemission studies,[33] 6–20 states/eV spin

TABLE I. Raman-active mode frequencies (ω), widths (Γ), and depolarization ratios (ρ) for Rb_3C_{60} and K_3C_{60} at $T=300$ K.

Mode	C_{60} ω	C_{60} Γ	C_{60} ρ	Rb_3C_{60} ω	Rb_3C_{60} Γ	Rb_3C_{60} ρ	$\Delta\Gamma_i/\omega_i^2$ (10^{-5} cm)	K_3C_{60} ω	K_3C_{60} Γ	K_3C_{60} ρ	$\Delta\Gamma_i/\omega_i^2$ (10^{-5} cm)
$H_g(1)$	270	4.2	0.52	268[a]	8.5	0.48	5.98	271[a]	12.5	0.74	11
$H_g(2)$	430.5	5.5	0.40	395	74		44	416	75	0.5	40
				476	7			479	0.6		
$A_g(1)$	493	2.5	0.02	494.5	0.1	0.04[b]		497	4.7	0.02	
$H_g(3)$	708	7.5	0.40	710	6			709	54		9.3
$H_g(4)$	773	9.0	0.38	741	57		8.7	750	64	0.63	9.4
$H_g(5)$	1099	7									
$H_g(6)$	1248	7									
$H_g(7)$	1426	7.5	0.44					1415	34		1.3
$A_g(2)$	1469	1.5	0.10	1448	4.3	0.04[b]	0.13	1453	9	0.18	0.36
$H_g(8)$	1573	9.5	0.52					1555	54	0.52	1.8
$\Sigma_i\Delta\Gamma_i/\omega_i^2$							59.0				73.0

[a]Least-squares fit to a BWF line shape where ω is the renormalized frequency.
[b]Close to the instrumental leakage level (~ 3–4 %).

C_{60} from band calculations,[34–38] and 10–15 states/eV spin C_{60} from NMR studies.[39]

Before discussing our values for T_c calculated according to Eq. (2), we first compute λ using $N(\varepsilon_F)=15$ states/eV spin C_{60}. Accordingly, we arrive at the value $\lambda=0.5$ (0.6) for Rb_3C_{60} (K_3C_{60}), which compares very favorably with the theoretical value by Schlüter *et al.*,[15] who obtained $\lambda=0.60$. Other groups have also examined the connection between the broadened Raman-active lines in M_3C_{60} and λ. Pichler *et al.*[40] reported the value $\lambda=0.002$ form the contribution due to the $A_g(2)$ mode. Mitch, Chase, and Lannin[10] reported a value of $\lambda=0.2$ obtained from the linewidth increase of the $H_g(2)$ mode which exhibits a dominant contribution to λ.

Returning to Eq. (2) and estimates of T_c from the Raman-mode broadening, we focus on the Rb_3C_{60} data in Table I which correspond to a sample for which we have also verified superconductivity at $T_c=28$ K. Using the parameter values given above, we obtain an estimate for $T_c=17$ K for Rb_3C_{60} from the McMillan equation [Eq. (2)] and the electron-phonon coupling constant λ derived from the Raman-active modes. We should point out that there may be several H_g-derived modes in the M_3C_{60} spectrum that are too broad to detect, and therefore are not included in our estimate for λ. However, these modes are the higher-frequency H_g modes, which, according to Eq. (1), makes a less important contribution to λ because of the $1/\omega^2$ weighting factor.

In Fig. 4, we compare the $T=300$ and 15 K Raman spectra for the same Rb_3C_{60} film. The inset in the upper left-hand corner in Fig. 4 shows the resistivity $\rho(T)$ for this particular film. A transition tempeature $T_c\sim28$ K can be obtained from $\rho(T)$. As can be seen in the figure, the Raman spectrum exhibits very little temepature dependence over this range. However, all these mode frequencies satisfy the relation $\omega>2\Delta=105$ cm^{-1},[12,13] and most of these modes are not expected to be sensitive to the superconductng transition, consistent with observations in the cuprates.[30]

Finally, we close our discussion with a few comments about the origin of the BWF line shape obseved for the $H_g(1)$ mode (Fig. 2). This line shape arises because of a coupling of the discrete $H_g(1)$ mode to a Raman-active continuum, which could be electronic in origin.[41,42] The line shape is given by

$$I=I_0\left[1+\frac{\omega-\omega_0}{\Gamma}\frac{1}{q}\right]^2\Big/\left[1+\frac{(\omega-\omega_0)^2}{\Gamma^2}\right], \qquad (3)$$

where ω is the renormalized discrete phonon frequency, $1/q$ is the strength of the coupling strength between the continuum and the discrete mode, and Γ is the width of the resonant interference between the continuum and discrete scattering channels. The value $1/q$ could be a measure of the coupling strength of the $H_g(1)$ mode to the t_{1u} electrons, if the continuum is indeed electronic rather than vibrational. It is interesting to note that the values of $1/q$ obtained here for M_3C_{60} ($1/q=-0.21$ for K_3C_{60} and $1/q=-0.38$ for Rb_3C_{60}) using the BWF analysis are comparable to those obtained similarly in the superconducting cuprates,[30] where $1/q$ was found in the range -0.2 to -0.5. The negative values obtained here for $1/q$ indicate that the center frequency of the continuum lies below the discrete mode frequency. Of course, it is also possible to fit the $\sim$268-cm^{-1} $H_g(1)$ line in the M_3C_{60} compounds by a six-parameter, two-Lorentzian line-shape function. This procedure might be appropriate if one attributes the features to two modes, split by a crystal field or Jahn-Teller interaction. The result of a least-squares line-shape analysis with unrestricted adjustment of all six parameters is $I_0(1)=40$, $\omega(1)=235$ cm^{-1}, $\Gamma(1)=50$ cm^{-1} and $I_0(2)=180$, $\omega(2)=263$ cm^{-1}, $\Gamma(2)=12$ cm^{-1}. Here I_0, ω, and Γ represent, respectively, the strength, frequency, and width of a Lorentzian line.

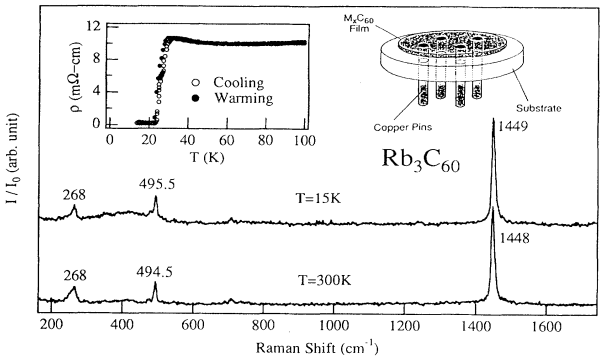

FIG. 4. Raman spectra of a superconducting Rb_3C_{60} film at $T=300$ and ~15 K. Inset: the schematic illustration of the sample on a substrate with copper pin electrodes (upper right corner) and the resistivity $\rho(T)$ (upper left corner).

SUMMARY AND CONCLUSIONS

Raman-scattering studies of films of M_3C_{60} (M=Rb,K) have been carried out. The spectra are found to be insensitive to the particular alkali-metal dopant, indicating that complete charge transfer has occurred. The electron-phonon coupling constant λ has been invoked to explain the broadening of the $H_g(2)$-$H_g(8)$ and $A_g(2)$ modes relative to their values in pristine C_{60} films. The $A_g(1)$-derived mode, on the other hand, actually narrows with M doping significantly, indicating a decrease in anharmonicity in the M_3C_{60} compounds. Experimental values for $\lambda\sim0.5$–0.6 are obtained which are in good agreement with a recent calculation by Schlüter *et al.*[7]

ACKNOWLEDGMENTS

The authors would like to thank Dr. A. M. Rao for helpful discussion. This work was made possible by the financial support from the Center for Applied Energy Research at the University of Kentucky. Research at MIT was supported by the National Science Foundation (No. 92-01878-DMR).

[1]A. F. Hebard *et al.,* Nature **350**, 600 (1991).
[2]M. J. Rosseinsky *et al.,* Phys. Rev. Lett. **66**, 2830 (1991).
[3]S. P. Kelty *et al.,* Nature **352**, 223 (1991).
[4]K. Tanigaki *et al.,* Nature **352**, 222 (1991).
[5]C. M. Varma *et al.,* Science **254**, 989 (1991).
[6]R. A. Jishi *et al.,* Phys. Rev. B **45**, 6914 (1992).
[7]M. Schlüter *et al.,* Phys. Rev. Lett. **68**, 526 (1992).
[8]K. H. Johnson *et al.,* Physica C **183**, 319 (1991).
[9]S. J. Duclos *et al.,* Science **254**, 1625 (1991).
[10]M. G. Mitch, S. J. Chase, and J. S. Lannin, Phys. Rev. Lett. **68**, 883 (1992).
[11]P. Zhou *et al.,* Phys. Rev. B **45**, 10 838 (1992).
[12]Z. Zhang *et al.,* Nature **353**, 333 (1991).
[13]Z. Zhang, C. C. Chen, and C. M. Lieber, Science **254**, 1619 (1991).
[14]A. Oshiyama and S. Saito, Solid State Commun. **82**, 41 (1992).
[15]M. Schlüter *et al.,* J. Phys. Chem. Solids **53**, 1473 (1992).
[16]A. F. Hebard, Phys. Today **45** (11), 26 (1992).
[17]C.-C. Chen and C. M. Lieber, J. Am. Chem. Soc. **114**, 3141 (1992).
[18]A. P. Ramirez *et al.,* Phys. Rev. Lett. **68**, 1058 (1992).
[19]T. M. Ebbesen *et al.,* Nature **355**, 620 (1992).
[20]S. Chakravarty *et al.*, Science **256**, 1306 (1992).
[21]K. Prassides *et al.,* Nature **354**, 462 (1991).
[22]W. Krätschmer *et al.,* Naure **347**, 354 (1990).
[23]P. C. Eklund *et al.,* J. Phys. Chem. Solids **53**, 1391 (1992).
[24]R. C. Haddon *et al.,* Nature **350**, 320 (1991).
[25]X. D. Xiang *et al.,* Science **256**, 1190 (1992).
[26]P. Zhou *et al.,* Phys. Rev. B **46**, 2595 (1992).
[27]P. C. Eklund *et al.,* Mater. Sci. Eng. B **19**, 154 (1993).
[28]($\|$,$\perp$): The incident laser radiation was polarized horizontally and the Raman-scattered light was polarized vertically.
[29]Z. H. Dong *et al.,* Phys. Rev. B **48**, 2862 (1993).
[30]S. L. Cooper and M. V. Klein, Comments Condens. Mater. Phys. **15**, 99 (1990).
[31]P. B. Allen, in *Dynamical Properties of Solids,* edited by G. K. Horton and A. A. Maradudin (North-Holland, New York, 1980), Vol. 3, p. 95.
[32]M. S. Dresselhaus, G. Dresselhaus, and P. C. Eklund, J. Mater. Res. **8**, 2054 (1993).
[33]C. T. Chen *et al.,* Nature **352**, 603 (1991).
[34]R. C. Haddon, L. E. Brus, and K. Raghavachari, Chem. Phys. Lett. **125**, 459 (1986).
[35]J. H. Weaver *et al.,* Phys. Rev. Lett. **66**, 1741 (1991).
[36]Q. Zhang, Y. J. Yi, and J. Berhnolc, Phys. Rev. Lett. **66**, 2633 (1991).
[37]S. Saito and A. Oshiyama, Phys. Rev. Lett. **66**, 2637 (1991).
[38]B. P. Feuston *et al.,* Phys. Rev. B **44**, 4056 (1991).
[39]R. Tycko *et al.,* Science **253**, 701 (1991).
[40]T. Pichler *et al.,* Phys. Rev. B **45**, 13 841 (1992).
[41]P. C. Eklund, M. S. Dresselhaus, and G. Dresselhaus, Phys. Rev. B **16**, 3330 (1977).
[42]P. C. Eklund and K. R. Subbaswamy, Phys. Rev. B **20**, 5157 (1979).